Dissection of angiogenic signaling in zebrafish using a chemical genetic approach

Joanne Chan,[1,3] Peter E. Bayliss,[1] Jeanette M. Wood,[2] and Thomas M. Roberts[1]

[1]Department of Cancer Biology, Dana-Farber Cancer Institute and the Department of Pathology, Harvard Medical School, Boston, Massachusetts
[2]Oncology Research, Novartis Pharma AG, CH-4002 Basel, Switzerland
[3]Correspondence: jochan@mbcrr.harvard.edu

Summary

Striking homology between signaling molecules in zebrafish and humans suggests that compounds known to inhibit human kinases may enable a chemical genetic approach to dissect signaling pathways in the zebrafish embryo. We tested this hypothesis using a vascular endothelial growth factor receptor inhibitor, PTK787/ZK222584. Zebrafish embryos treated with this compound lacked all major blood vessels. Overexpression of AKT/PKB, a putative effector of vascular endothelial growth factor signaling, allowed blood vessels to form in the presence of drug. Endothelial cell apoptosis induced by the drug is prevented by increasing AKT/PKB activity, thus establishing the physiological relevance of AKT/PKB in the angiogenic process. This approach allowed us to examine the effects of blood flow and the role of endothelial signals in organogenesis.

Introduction

Our current knowledge on the physiological function of various genes has benefited from studies using model organisms. Although informative, targeted gene disruption in mice blocks function at such an early stage that it sometimes hinders the ability to learn about gene function at later stages of development. While conditional loss-of-function experiments are possible in the mouse (reviewed in Lewandoski, 2001; Mills, 2001), these technologies do not allow much flexibility in and control over residual gene function. In other model organisms, such as *Drosophila* and *C. elegans*, the use of a controlled modulation of gene dosage by temperature-sensitive and partial loss-of-function alleles has generated valuable information on signaling pathways (reviewed in Rubin, 1991; Simon et al., 1991; Sternberg, 1993; Sternberg and Horvitz, 1991). However, invertebrates do not possess the extensive circulatory and other organ systems of vertebrates, making them less than ideal for the study of more complex processes such as angiogenesis and organ development.

The zebrafish provides an alternative vertebrate model system. The fish possesses a complex circulatory system similar to that of mammals, as well as reasonable counterparts for many, although not all, of the other mammalian organ systems (Kimmel et al., 1995; Isogai et al., 2001; Fishman, 2001; Thisse and Zon, 2002). The rapid external development of the transparent zebrafish embryo permits easy visual analysis of phenotypic defects. Currently, the simplest method for generating a loss-of-function in a particular gene in the zebrafish is the use of antisense technology using morpholino oligonucleotides to induce a translational block in gene function (Nasevicius and Ekker, 2000; Ekker, 2000). Although important information can be obtained by morpholino injections, this method, similar to the use of null mutations, blocks gene function at the earliest stage. We set out to use a novel strategy to study signal transduction in the zebrafish embryo using a chemical genetic approach to achieve a rheostatic control of signal strength. We used this strategy to study angiogenic signaling in the transparent zebrafish embryo.

The need for new blood vessels is important during embryogenesis, as well as in pathological situations such as tumor growth (reviewed in Carmeliet and Jain, 2000). Thus, the molecular dissection of angiogenic signaling is clinically relevant. The formation of blood vessels and evaluation of blood flow is extremely easy to score in the zebrafish embryo, making it an ideal model for the study of angiogenesis. The major regulators of angiogenic signaling, the vascular endothelial growth factors (VEGFs) and their receptors (VEGFRs), promote endothelial cell differentiation, survival, and migration (reviewed in Carmeliet, 2000; Ferrara and Alitalo, 1999). By addition of a kinase inhibitor targeted against the VEGF receptors to the media bathing the fish embryo, we phenocopied the loss of VEGF ligand function

SIGNIFICANCE

Our work represents a novel strategy to study signal transduction using a chemical genetic approach in an intact vertebrate organism. The use of a chemical compound to dissect angiogenic signaling has allowed fine tuning of effective gene dosage. As in other genetic models, such as *Drosophila*, we were able to bypass the receptor blockade by upregulating the activity of a putative downstream effector, AKT/PKB. The combination of chemical genetics and the transparent zebrafish embryo can be used to study other signal transduction pathways as well as for drug evaluation. The assays we have employed here are both inexpensive and facile relative to mouse studies, suggesting that the zebrafish may be used as a preclinical model for drug testing.

brought about by morpholino injections, where blood vessel formation was prevented (Nasevicius et al., 2000). The chemically induced VEGF receptor defect can be ameliorated by upregulating the activity of a putative downstream effector, AKT/PKB, allowing for normal endothelial cell functions in migration and survival.

Results

Molecular rationale for using a VEGF receptor inhibitor in zebrafish

Preliminary to drug testing, we cloned and sequenced the full-length zebrafish cDNAs for VEGFR-2/flk-1/KDR as well as for several key members of its downstream signaling apparatus, including PI3-kinase (p110α and p85α), PTEN, and AKT-2/PKBβ, and found high overall homology to their human counterparts (Figure 1 and J.C. and T.M.R., unpublished data). The zebrafish VEGFR-2/flk-1/KDR cDNA is the full-length version of the partial cDNAs previously reported by several other groups (Fouquet et al., 1997; Liao et al., 1997; Sumoy et al., 1997; Thompson et al., 1998). The high level of conservation in the tyrosine kinase domain between human and zebrafish VEGFR-2 (78% identity, Figure 1A) provided a structural basis for use of the antiangiogenic compound PTK787/ZK222584 on zebrafish embryos.

Specific angiogenic inhibition by PTK787/ZK222584 phenocopies functional loss of VEGF-A ligand

PTK787/ZK222584 is a novel anilinophthalazine compound and a high affinity inhibitor of the VEGF receptors, with a higher potency toward VEGFR-2/KDR than VEGFR-1/Flt-1 (IC_{50} = 37 nM and 77 nM, respectively; Wood et al., 2000). Although it also exhibits inhibitory activity toward the PDGF, Flt-4, and c-Kit receptors, this occurs at higher concentrations (Wood et al., 2000; Bold et al., 2000). Previous studies have shown the effectiveness of this drug in cell culture and in murine retina neovascularization and carcinoma models (Wood et al., 2000; Bold et al., 2000; Drevs et al., 2000; Ozaki et al., 2000). We first tested the effectiveness of this compound on the zebrafish VEGFR-2 receptor expressed in vitro in mammalian cells, where ligand-induced autophosphorylation of the zebrafish receptor was inhibited by PTK787/ZK222584 at approximately the same concentrations used on the mammalian VEGF receptors (Figure 1B). Treatment of live fish embryos with PTK787/ZK222584 completely blocked the formation of all major blood vessels at a concentration of 5 μM in fish embryo media (Figure 2 and Table 1). At 1 μM, we observed a 34% vessel inhibition in our system (Table 1), which may be compared to its use at plasma concentrations above 1 μM in mouse tumor studies (Wood et al., 2000; Drevs et al., 2000; Ozaki et al., 2000). The PTK787/ZK222584-induced antiangiogenic phenotype is remarkably similar to the loss of VEGF-A ligand function produced by antisense morpholino targeting (Figures 2A–2D; Nasevicius et al., 2000). Embryos treated with PTK787/ZK222584 showed a complete blockade of blood vessel formation as the dorsal artery and posterior cardinal vein fail to form by 48 hr of development (Figures 2G–2J). This results in severe pericardial edema (Figure 2D), with further complications of heart failure and embryonic death by 3 days of development. The lack of deleterious effects on the general morphology of embryonic structures by 24 hpf

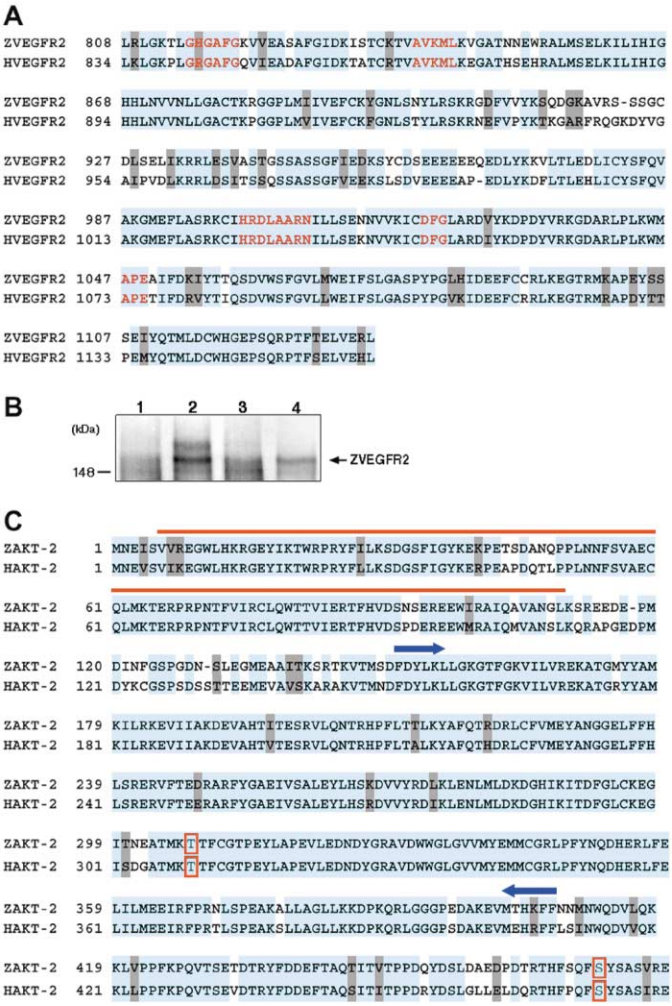

Figure 1. Molecular basis for chemical inhibition and VEGF pathway conservation

A: Sequence comparison of the predicted protein-tyrosine kinase domain, residues 808 to 1134 of zebrafish (top) with human (bottom) VEGFR-2. Hallmark residues of kinase subdomains I, II, VI, VII, and VIII are indicated by red letters. **B:** Expression and chemical inhibition of the zebrafish VEGFR-2 receptor by PTK787/ZK222584 in mammalian cells. Lane 1, vector-transfected COS cell lysates; lanes 2–4, zebrafish VEGFR-2-transfected COS cell lysates. COS cells in lanes 1, 2, and 3 were stimulated with zebrafish VEGF-A ligand. Cells in lane 3 were preincubated with 100 nM PTK787/ZK222584 for receptor inhibition. Cells in lane 4 express the zebrafish VEGFR-2 receptor. Cell lysates were immunoprecipitated with anti-phosphotyrosine antibody and immunoblotted with the same antibody to show a tyrosine phosphorylated band of the expected size for the zebrafish VEGFR-2 receptor, ~180 to 200 kDa. **C:** Sequence alignment of predicted zebrafish (top) and human (bottom) AKT-2 protein. The PH domain is indicated by a red overline; the protein-serine/threonine kinase domain is indicated by blue arrows. The residues boxed in red correspond to Thr308 and Ser473 phosphorylation sites of human AKT-1. For both **A** and **B**, identical residues are boxed in blue, similar residues in gray. The full-length cDNAs encoding zebrafish VEGFR-2 and AKT-2 have been submitted to GenBank: *VEGFR-2/flk* (accession number AY056466), *AKT-2* (accession number AY056465); human sequences were taken from GenBank.

(Figures 2A and 2B) argues strongly for the selectivity of PTK787/ZK222584 for VEGF receptors. The potent antiangiogenic effect of PTK787/ZK222584 is further confirmed by a significant reduction of endothelial cells in the region of the

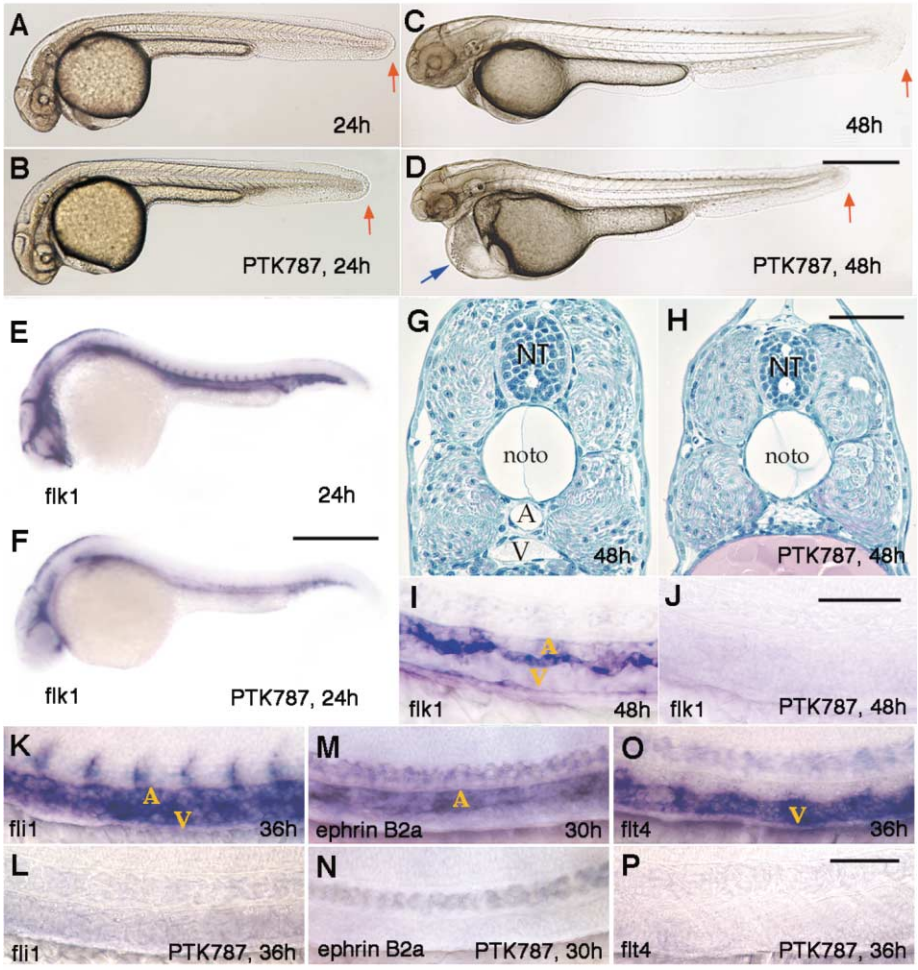

Figure 2. PTK787/ZK222584 treatment of live zebrafish embryos specifically inhibits angiogenesis

Zebrafish embryos were treated at shield stage (60% epiboly, 6 hpf) with PTK787/ZK222584 (**B**, **D**, **F**, **H**, **J**, **L**, **N**, and **P**, as indicated), and compared with same stage untreated embryos (**A**, **C**, **E**, **G**, **I**, **K**, **M**, and **O**, respectively). **A–D:** Lateral views of live embryos at 24 hpf (**A** and **B**) and 48 hpf (**C** and **D**). PTK787/ZK222584-treated embryos were shorter in length, as indicated by red arrows; the blue arrow in **D** indicates pericardial edema. **E, F, and I–P:** In situ RNA hybridization with various endothelial cell markers. *VEGFR-2/flk-1 RNA staining* of 24 hr embryos in **E** and **F**, 48 hr embryos in **I** and **J**. **G and H:** Hematoxylin-eosin/azure II staining of transverse sections of 48 hr embryos revealing the lumens of the dorsal artery, A, and vein, V, in the control embryo (**G**); and their absence in the PTK787/ZK222584-treated embryo (**H**). **I and J:** 48 hr embryos stained with the *VEGFR-2/flk-1* RNA probe, and flat-mounted at the level of the dorsal artery and posterior cardinal vein to show the absence of *VEGFR-2/flk-1*-positive endothelial cells in the drug-treated embryo (**J**). **K and L:** 36 hr embryos stained with the early endothelial marker *fli-1*. **M and N:** 30 hr embryos stained with the *ephrinB2a* marker for arterial endothelial cells. **O and P:** 36 hr embryos stained with the venous endothelial marker *flt4*. Endothelial cell staining is reduced or absent from all PTK787/ZK222584-treated embryos (**J**, **L**, **N**, and **P**). Abbreviations: PTK787, PTK787/ZK222584 treatment; NT, neural tube; noto, notochord; A, dorsal artery; V, posterior cardinal vein. Scale bars for **A–D** = 500 μm; **E** and **F** = 500 μm; **G** and **H** = 50 μm; **I** and **J** = 100 μm; **K–P** = 100 μm.

dorsal artery and posterior cardinal vein at 24 hpf, and by their absence at 48 hpf as indicated by *flk-1/VEGFR-2* in situ RNA staining (Figures 2E, 2F, 2I, and 2J). This is confirmed by the distinctive absence of these major blood vessels by 48 hpf when viewed in transverse section (Figures 2G and 2H). We analyzed this defect further using established endothelial markers: *fli1* for endothelial precursors (Figures 2K and 2L; Thompson et al., 1998) and *ephrin B2a* for arterial endothelial cells (Figures 2M and 2N; Chan et al., 2001), as well as *flt4* for venous endothelial cells (Figures 2O and 2P; Thompson et al., 1998). In all cases, endothelial cell staining was either abolished or significantly reduced in the region of the major dorsal vessels in the PTK787/ZK222584-treated animal, as compared with same stage controls (Figures 2I–2P).

Since early administration of PTK787/ZK222584 resulted in zebrafish embryos that do not possess an intact dorsal artery or vein and have no aortic blood flow, it prompted us to examine organogenesis in treated animals (Serluca et al., 2002; Lammert et al., 2001; Matsumoto et al., 2001). During kidney formation, intermediate mesoderm precursor cells expressing the Wilms' tumor suppressor gene (*wt1*) migrate toward the midline and coalesce around a vascular sprout from the aorta to form the glomerulus (Serluca and Fishman, 2001). These cells mark the bilateral pronephric primordia by 36 hpf (Figure 3A) that develop into the midline glomerulus by 48 hpf (Figure 3B). In the zebrafish, a strict requirement for blood flow determines proper glomerular assembly (Serluca et al., 2002). The lack of aortic blood flow in embryos treated at early stages with PTK787/ZK222584 generated defects in glomerulogenesis, as *wt1*-positive cells remain unmerged at 48 hpf and beyond (Figures 3D–3F). However, later administration of drug, after the onset of aortic flow by 26 hpf, allowed for glomerular assembly, demonstrating that PTK787/ZK222584 does not illicit a deleterious effect on kidney development on its own (Figure 3C). We also examined the development of the endocrine pancreas (*insulin*; Figures 3G and 3H; Milewski et al., 1998; Argenton et al., 1999), the exocrine pancreas (*trypsin*, Figures 3I and 3J; Biemar et al., 2001) as well as the liver (*fkd2*; Figures 3K and 3L; Chen et al., 2001) using established in situ markers. In spite of the dramatic reduction of endothelial cells (Figures 2E–2P), all markers are expressed (Figures 3G–3L). However, the expression domains for *trypsin* and *fkd2* appear shortened along the anterior-posterior axis (Figures 3I–3L).

Use of chemical genetics allows precise temporal and dosage control of receptor inhibition

Unlike antisense targeting strategies, this antiangiogenic compound can be administered at any stage of development to block the formation of particular blood vessels as they develop during the first few days of embryonic and larval life (data not

Table 1. Analysis of angiogenic phenotypes in live zebrafish embryos

Antiangiogenic effects of PTK787/ZK222584 at various concentrations[a]

PTK787 concentration	Dorsal artery absent	Dorsal artery present	Number
10 μM	100%	0%	200
5 μM	100%	0%	200
2.5 μM	81%	19%	220
1 μM	34%	66%	200
0.5 μM	6%	94%	200
0.25 μM	0%	100%	200

Antiangiogenic effects of 10 μM PTK787/ZK222584[b] at various stages

Embryo stage at treatment	Mild defect[c]	Moderate defect[d]	Severe defect[e]	Death	Number
1-cell to 18S	0%	0%	90%	10%	200
24 hpf	0%	0%	95%	5%	200
30 hpf	26%	25%	49%	0%	200
36 hpf	78%	17%	5%	0%	200

AKT-mediated blood vessel recovery upon VEGF receptor or ligand inhibition

Experimental conditions	Good recovery[c]	Moderate recovery[d]	Poor recovery[e]	Number
PTK787 treatment and washout[f]				
Uninjected embryos	8%	25%	67%	200
AKT injected embryos	37%	29%	34%	200
GFP injected embryos	6%	32%	62%	200
No treatment	100%	0%	0%	200
VEGF morpholino injections[g]				
VEGF morpholino	0%	19%	81%	200
VEGF morpholino + AKT	12%	41%	47%	200

[a] Embryos were treated at 60% epiboly and staged according to Kimmel et al. (1995).
[b] Observations were recorded at 48 hpf.
[c] Intersegmental vessels at >50% the normal number.
[d] Intersegmental vessels at 30–50% the normal number.
[e] Intersegmental vessels at <30% the normal number.
[f] Embryos were treated at 24 hpf, with 10 μM of PTK787/ZK222584. Drug was washed out at 30 hpf and embryos were examined at 48 hpf.
[g] Embryos were injected with either VEGFA3 morpholino alone or in combination with myrAKT mRNA at the one-cell stage and examined at 52 hpf.
Abbreviations: PTK787, PTK787/ZK222584; 18S, 18-somites; hpf, hours postfertilization.

shown). From 24 hpf to 48 hpf, the development of the intersegmental vessels in the zebrafish can be easily visualized using live embryo microangiography (Weinstein et al., 1995; Isogai et al., 2001), where a fluorescent dye is injected into the embryonic circulation (Figure 4). When embryos are treated with PTK787/ZK222584 after the establishment of blood flow in the dorsal artery and cardinal vein at 24 hpf, the intersegmental vessels fail to form (Table 1).

Since PTK787/ZK222584 is a reversible competitor, we performed drug washout experiments where embryos were treated with the compound from 24 hpf to 30 hpf, after which the drug was removed by serial washes in embryo media before an incubation period in drug-free embryo media (Figure 4C and Table 1). We observed that after drug removal, some intersegmental vessels are formed. However, these rescued vessels are markedly fewer in number as compared with same-stage control embryos (Figures 4B and 4C).

Overexpression of the downstream effector AKT/PKB can rescue VEGF receptor blockade

In *Drosophila* genetics it has been possible to tentatively establish the order of signaling molecules in a pathway by rescuing a partial loss of function mutation in one component by upregulating the activity of a downstream component. Recent evidence suggests a role for PI 3-kinase and PTEN in angiogenic signaling (Jiang et al., 2000; Wen et al., 2001). In particular, cell culture studies have suggested a role for AKT/PKB as a downstream effector of VEGF signaling (Gerber et al., 1998; Fujio and Walsh, 1999). In addition to the optical transparency of the embryo, the zebrafish is also amenable to mRNA microinjection experiments, which permit exogenous expression of activated forms of intracellular proteins. We tested whether overexpression of AKT/PKB, a putative downstream element, could rescue drug-induced loss of receptor function by microinjecting embryos at the one-cell stage with myristoylated-AKT/PKB mRNA prior to PTK787/ZK222584 treatment. As the conservation in the PI 3-kinase pathway between fish and man is generally high (Figure 1C; Chan and Roberts, in preparation), we decided to use a constitutively activated version of human AKT-1/PKBα (Ramaswamy et al., 1999) in our analysis. We observed much faster and more efficient recovery of intersegmental vessels in drug washout experiments in embryos overexpressing activated AKT/PKB as compared with uninjected controls (Figures 4C and 4D, Table 1), while a kinase-dead version of myristoylated-AKT/PKB was unable to override the receptor defect (Figure 5). We also tested the ability of another potential downstream effector, endothelial nitric oxide synthase (eNOS), which is preferentially expressed in endothelial cells and known to participate in VEGF receptor signaling in cultured cells. Phosphorylation of bovine eNOS by AKT/PKB at Ser1179 (Ser1177 in human eNOS) has been shown to upregulate its activity (Fulton et al., 1999; Dimmeler et al., 1999). Using mRNA encoding either an activated form of eNOS (S1179D, which mimics the AKT/PKB phosphorylation) or an AKT/PKB-resistant version, S1179A, in drug washout experiments, we observed a modest rescue in the number of intersegmental vessels with the activated version of eNOS. The rescue was statistically significant but not as robust as that seen with AKT/PKB (Figure 5 and Table 1).

Experiments in cultured endothelial cells suggest that the overexpressed AKT/PKB could be acting, at least in part, by preventing endothelial cell apoptosis (Gerber et al., 1998; Fujio and Walsh, 1999), but we wondered if our mRNA injections were having more global effects on cell survival. To investigate this, we determined the extent of apoptosis in whole-mount TUNEL assays (Figure 6). In control embryos, we observed the naturally occurring apoptosis in the neural tube at 48 hpf (Figures 6A and 6B). When embryos are treated with drug after the establishment of blood flow by 24 hpf, the amount of apoptotic cell death in the region of the dorsal artery and vein is dramatically increased (Figures 6C and 6D). In contrast, when embryos overexpressing activated AKT/PKB are exposed to the same drug treatment, the amount of apoptotic cell death is reduced to background levels in the region of the blood vessels (Figures 6E and 6F). However, exogenous AKT/PKB activity did not appear to have a protective effect on the normal apoptosis in the neural tube. The specificity of PTK787/ZK222584 effects on endothelial cells is underscored by comparison with wortmannin treatment of live embryos, where a high level of apoptotic cell death was observed throughout the embryo (Figures 6G and 6H).

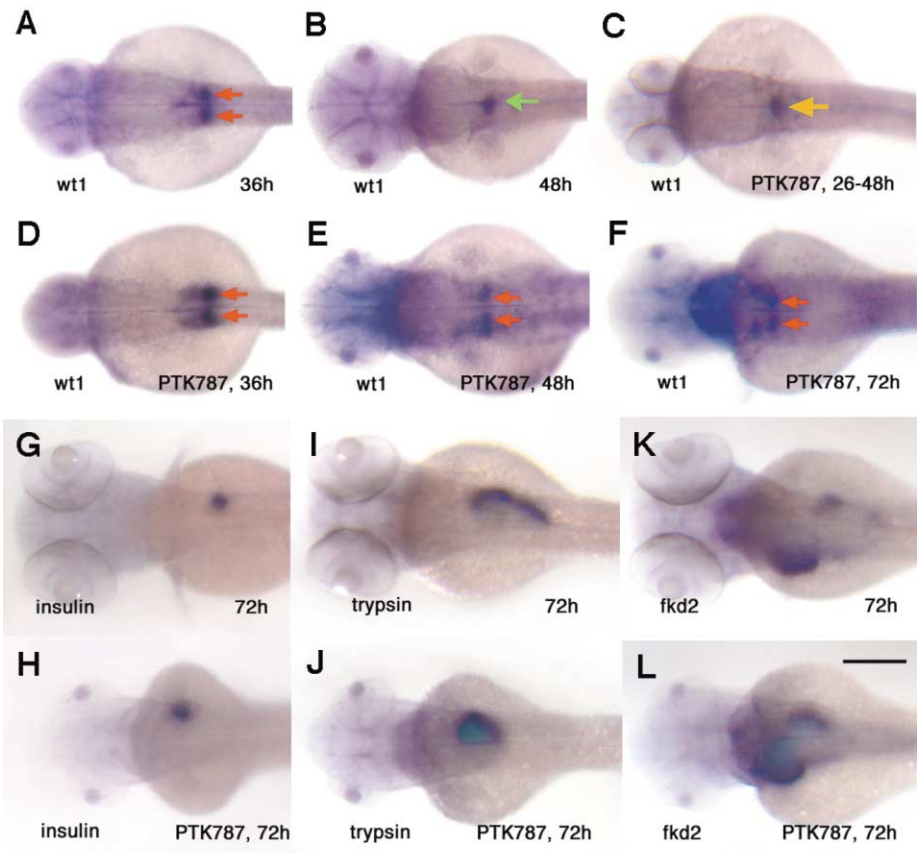

Figure 3. Organogenesis in PTK787/ZK222584-treated zebrafish embryos

Antisense RNA staining of whole-mount embryos, dorsal views with anterior to the left in all panels. **A–F:** Kidney glomerular assembly was examined using the *wt1* probe. Control embryos at 36 hr (**A**) and 48 hr (**B**) stained with *wt1* show the migration of the bilateral podocytes (red arrows) toward the midline where fusion occurs by 48 hpf as indicated by the green arrow. When embryos are treated with PTK787/ZK222584 at shield stage (60% epiboly, 6 hpf) before aortic blood flow, the *wt1*-positive cells do not fuse at the midline (**D**, **E**, and **F**). PTK787/ZK222584-treatment after aortic flow at 26 hpf in **C**. Migration of *wt1*-positive podocytes toward the midline appears unaffected. **G–L:** *insulin*, *trypsin,* and *fkd2* staining of control (**G**, **I**, and **K**) and PTK787/ZK222584-treated (**H**, **J**, and **L**) embryos, showing the locations of the endocrine pancreas, the exocrine pancreas, and the liver, respectively. Abbreviations: PTK787, PTK787/ZK222584 treatment. Scale bar for all panels indicates 200 μm.

Inhibitors of serine/threonine kinases can phenocopy known defects

To see if the zebrafish could be used to study both tyrosine and serine/threonine kinase inhibitors, we also tested the effectiveness of a broad spectrum protein kinase C inhibitor, PKC412 (Meyer et al., 1989), and an inhibitor of MEK, U0126 (Favata et al., 1998). Treatment of zebrafish embryos with PKC412 generated a distinctive curvature of the body axis which phenocopies that of the genetic zebrafish mutant, *heart and soul* (*has*) (Stainier et al., 1996; Figures 7A–7D). Recent work has shown that the *has* mutant harbors stop codons in the coding region of an atypical protein kinase C gene, *PKC*λ (Peterson et al., 2001; Horne-Badovinac et al., 2001). Treatment of fish embryos with a Mek inhibitor, U0126, induced a specific loss of posterior structures which phenocopies the published effects of expression of a dominant-negative Raf in the *Xenopus* (Figures 7E and 7F; MacNicol et al., 1993). To examine the effects of these compounds on zebrafish angiogenesis, we performed in situ RNA staining with the endothelial marker *flk-1* (Figures 7G–7J). At 24 hpf, PKC412-treatment did not significantly reduce endothelial cell staining as compared with control or *has* embryos (Figures 7G–7I). Thus, PKC412 did not generate antiangiogenic effects as PTK787/ZK222584 when used on live zebrafish embryos in the same treatment regime (Figures 7G–7I; Figure 2). Similar examination of U0126 effects showed that endothelial cells are present but their expression domain is deformed (Figure 7J). The morphological changes in *flk-1*-positive cells are likely secondary to the gross deformity in the trunk (Figures 7E and 7F).

Discussion

The use of an inhibitor in place of the classic loss-of-function mutation allows us to perform experiments which would be extremely difficult or impossible in the fish using either mutations in the VEGF receptors or downregulation via antisense or RNA interference technology. During the development of the vertebrate organism, the exact timing of developmental events is crucial to the formation of tissues and organ systems. A chemical genetic approach permits both temporal and dosage control over the modulation of gene function, allowing precise initiation and termination of the functional blockade (Peterson et al., 2000, 2001). Controlled administration of PTK787/ZK222584 inactivated VEGF receptors at the most important time in the angiogenic process. In addition, the drug also allows us to block multiple receptor alleles in one facile step.

To study signaling components in this pathway, we borrowed an idea from *Drosophila* studies where genetic rescue of a hypomorphic allele is commonly used in pathway mapping (Simon et al., 1991). We reasoned that when the VEGF receptor was impaired, a low level activity of a downstream component might provide just enough pathway activation to achieve the signaling threshold necessary for endothelial cell function. Previous work in cultured endothelial cells has shown that the AKT/PKB branch of PI 3-kinase signaling is essential for VEGF-medi-

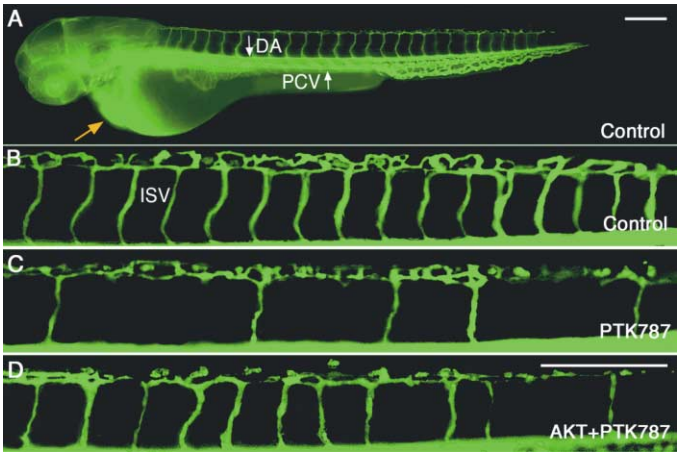

Figure 4. Microangiography of live zebrafish embryos following PTK787/ZK222584-treatment and drug washout experiments

Live zebrafish embryos at 2 days of development were injected with a fluorescent lectin dye and circulation was visualized using an epifluorescence microscope. **A:** Microangiograph of the circulation in a control untreated embryo within minutes of dye injection into the pumping embryonic heart, indicated by the orange arrow. **B–D:** Higher magnification of the same stage embryos focusing on the intersegmental vessels along the trunk of the embryo. The control embryo (**B**) shows a regular spacing of intersegmental vessels. **C and D:** After the establishment of flow in the dorsal artery and posterior cardinal vein at 24 hpf, embryos were treated with PTK787/ZK222584 for a period of 6 hr, the drug was washed out at 30 hr, and the embryos were allowed to recover until 48 hpf before microangiography. Note the reduced number of intersegmental vessels in **C**. Embryo in **D** was injected with myristoylated-AKT/PKB mRNA at the one-cell stage before drug treatment, and displayed more vessels. Abbreviations: PTK787, PTK787/ZK222584 treatment; AKT+PTK787, injected with AKT/PKB mRNA before PTK787/ZK222584 treatment; DA, dorsal artery; PCV, posterior cardinal vein; ISV, intersegmental vessel. Scale bars for **A** = 200 μm; **B**–**D** = 200 μm.

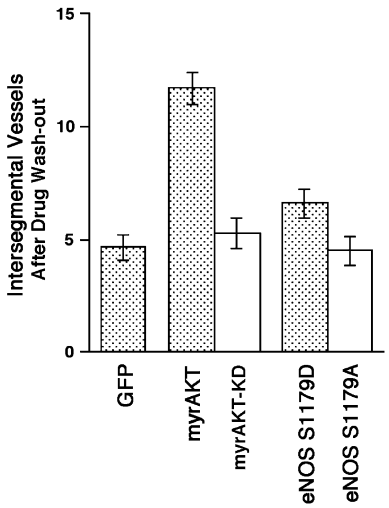

Figure 5. Comparison of AKT/PKB versus eNOS in vessel rescue

y axis indicates the mean number of intersegmental vessels per mRNA-injected embryo in PTK787/ZK222584 washout experiments as described. x axis indicates various mRNAs injected: GFP for control; myrAKT for myristoylated, activated AKT/PKB, myrAKT-KD for the kinase-dead version; eNOS S1179D for activated and eNOS S1179A for AKT/PKB resistant versions of eNOS. $n \geq 200$; $p < 0.0001$ by one-way analysis of variance. Error bars show the 95% confidence limits. Only myrAKT/PKB and eNOS S1179D show statistically significant differences ($p < 0.05$) from GFP-injected fish, both at $p < 0.0001$ by two-tailed unpaired t test.

ated cell survival and migration (Gerber et al., 1998; Fujio and Walsh, 1999; Morales-Ruiz et al., 2000). We tested the ability of AKT/PKB to provide a functional bypass in receptor blockage by looking at vessel recovery after a 6 hr exposure to PTK787/ZK222584. Judging by the number of intersomitic vessels formed after washout, we determined that a low level of exogenous AKT/PKB activity generated a much more robust rescue than in uninjected controls (see Table 1). Thus, endothelial cell function, in this case, as indicated by the ability to migrate into the intersomitic region and form functional vessels, is rescued in the presence of increased AKT/PKB activity (Figure 4 and Table 1). Since AKT/PKB is a molecule with ubiquitous expression and pleiotropic effects, we cannot rule out the possibility that AKT/PKB is acting in a pathway independent from the VEGF receptor signaling pathway. However, our data is much more easily explained by the simple hypothesis that rescue occurs for VEGF signaling. Notably, upregulated AKT/PKB activity was able to rescue the VEGF receptor defect created by the drug, but not the naturally occurring apoptosis in the neural tube. Since, by design, the 6 hr pulse of drug in washout experiments had been tailored to leave considerable residual VEGF receptor function, we would expect that the levels of AKT/PKB activity needed to rescue drug action would not be sufficient to rescue natural apoptosis. Unfortunately, we were not able to further test this hypothesis by raising AKT/PKB activity still higher in an attempt to rescue cell death in the neural tube, because at higher levels, AKT/PKB overexpression generated gastrulation defects. Our rescue experiments with eNOS yielded a statistically significant but very modest rescue (Figure 6 and Table 1). Since AKT/PKB is upstream of eNOS in its signaling pathway (Fulton et al., 1999; Dimmeler et al., 1999), it is perhaps not surprising that AKT/PKB generates a more robust rescue.

Our study serves to illustrate the interdependence of signal transduction research and inhibitor drug action. There is a certain reciprocity in the information flow arising from studying the interaction of potential drugs in zebrafish: the fish can give us information about compounds under study, but the compounds can also reveal the mechanisms regulating development. Highly specific inhibitors can help us immensely in elucidating signal transduction pathways, while the flaws of less specific compounds may be revealed by their effects on development. PTK787/ZK222584 is specific and hence has provided us valuable information about the VEGF receptor signaling pathway in angiogenesis and allowed us to examine the consequences of receptor inhibition on organ development in an intact organism. The absolute lack of blood flow that resulted from chemical inhibition at early stages prevented glomerulogenesis during kidney formation as predicted from previous studies (Figures 3A–3F; Serluca et al., 2002). The formation of the endocrine pancreas, as marked by *insulin* staining, does not appear different after drug treatment, suggesting that the lack of an intact aortic endothelium and blood flow is insufficient to alter pancreatic development at this stage. In studies in mouse and *Xenopus*, the development of the endocrine pancreas has been shown to depend on interactions with the endothelium (Lammert et al., 2001). It is possible that in the fish, endothelial interactions are not required for pancreatic development, or alternatively there

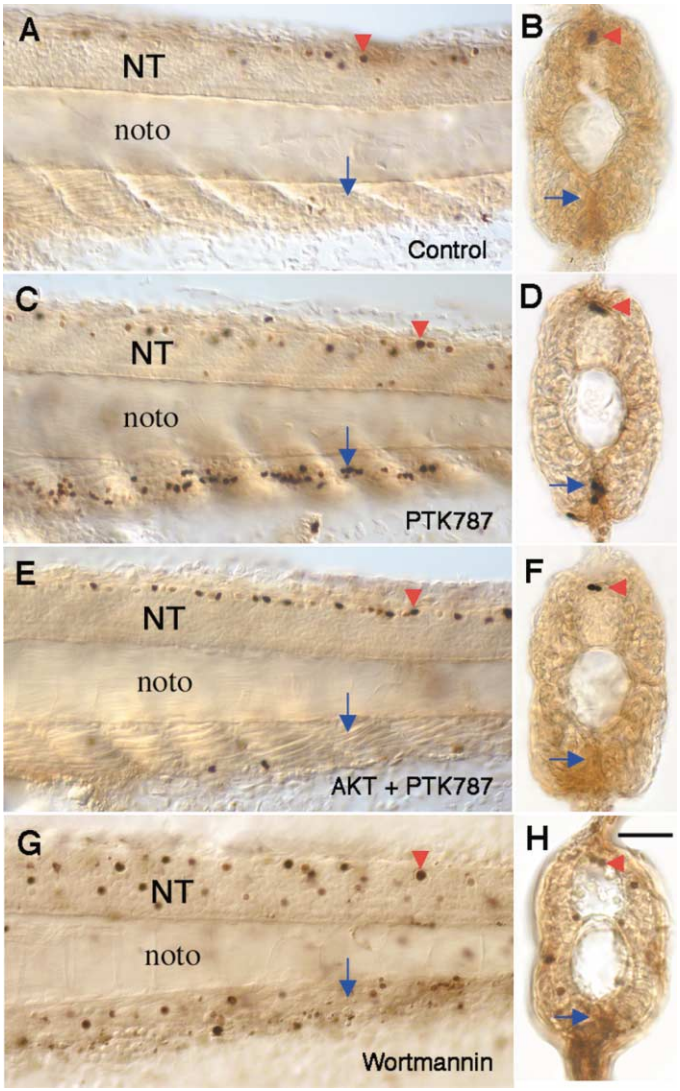

Figure 6. PTK787/ZK222584-induced endothelial cell apoptosis can be specifically prevented with overexpression of activated AKT/PKB

Whole-mount TUNEL assays were performed on untreated and PTK787/ZK222584-treated embryos. **A**, **C**, **E**, **and G:** Lateral views of flat-mounted embryos; **B**, **D**, **F and H:** manual cross-sections of the same embryos, respectively. **A and B:** Control untreated embryos showing endogenous apoptotic cell death along the neural tube, red arrowhead in all panels. **C–F:** Embryos were treated with PTK787/ZK222584 at 24 hpf and fixed at 48 hpf for TUNEL analysis. Exposure to PTK787/ZK222584 induced endothelial cell death at the region of the dorsal artery and posterior cardinal vein (**C** and **D**); blue arrows indicate position of endothelial cells in all panels. Embryos injected at the one-cell stage with myristoylated-AKT/PKB showed reduced apoptotic cell death in the endothelial cells, but apoptosis along the neural tube appears unaffected in **E** and **F**. Embryos were treated with 5 μM wortmannin at 24 hpf and fixed at 48 hpf for TUNEL analysis in the same manner in **G** and **H**. Scale bar for all panels indicates 50 μm.

may be a sufficient number of endothelial cells in drug treated fish to allow pancreas formation. In the zebrafish, the notochord, which is required for dorsal artery formation (Fouquet et al., 1997), does not appear to be a source of inductive signals in pancreatic development. The genetic mutant, floating head, *flh*, which lacks a notochord, still exhibits normal insulin expression in the proper morphological location (Biemar et al., 2001). The *flh* mutants, like our drug treated fish, still display limited numbers of endothelial cells (Fouquet et al., 1997), perhaps enough for induction of the endocrine pancreas. As recent data suggested a requirement for sonic hedgehog (shh) signaling in zebrafish pancreatic specification (Roy et al., 2001), we also confirmed that *shh* expression is not altered in our chemical inhibitions (data not shown). Although the general staining and morphological location of the endocrine and exocrine pancreas, as well as the liver primordia, appear to be correct, the expression domains of two of these markers are reduced along the anterior-posterior axis (Figures 3G–3L), suggesting that endothelial signals may be required for organ morphogenesis without affecting cellular differentiation. In the case of liver development, our preliminary analysis is consistent with that of Matsumoto et al. (2001) in *flk-1/VEGFR-2* null mice, which showed that specification of the liver does occur in the absence of vessels. These data suggest that our system can be further developed to explore developmental questions in organogenesis in an intact animal without surgical manipulation. Since signals between endothelial cells and developing tissues during organogenesis may be reprised during tumor angiogenesis, understanding these interactions may improve our understanding of cancer biology.

In these proof of concept experiments, the drug target was already known, but we feel that the system could be of value in determining the mechanisms of action of novel compounds. If PTK787/ZK222584 targets had been unknown, its potent antiangiogenic effects on the fish would have pointed to the correct pathway if not to the exact target. Our rescue experiment suggests that it may be possible to locate the target of a drug within a pathway by overexpressing various pathway members. In the course of this study, we have also tested serine/threonine kinase inhibitors, PKC412 and U0126, for their ability to induce specific phenotypes in the zebrafish. PKC412 generated a distinctive curvature of the body axis which phenocopied that of the genetic zebrafish mutant, *heart and soul* (*has*) (Stainier et al., 1996), which resulted from mutations in the protein kinase C gene, *PKC*λ (Peterson et al., 2001; Horne-Badovinac et al., 2001). In the case of MEK, drug inhibition phenocopies Raf-1 interference in *Xenopus* embryos (MacNicol et al., 1993).

Any study using small molecule inhibitors must address the issue of target specificity. For instance, PTK787/ZK222584 is known to inhibit the platelet-derived growth factor (PDGF) and the c-Kit receptors at higher concentrations (Bold et al., 2000; Wood et al., 2000). Inhibition of these receptors is unlikely to underlie our antiangiogenic phenotype since we would expect to see alterations in pigmentation if either receptor were being inhibited. Mutation of the c-*kit* gene in the zebrafish *sparse* mutant results in reduced melanocyte production (Parichy et al., 1999). From the *Patched* mutation in mice, we also expect that PDGF receptor inhibition would generate pigment defects (Smith et al., 1991; Stephenson et al., 1991). To address these concerns in a more general way, we used a VEGF ligand morpholino (Nasevicius et al., 2000) to block the VEGF receptor pathway. We were able to obtain a specific antiangiogenic phenotype that could, with some difficulty, be rescued by coinjection with myristoylated AKT/PKB mRNA (Table 1). By lowering the amount of VEGF-A morpholino injected, while adjusting the amount of myristoylated AKT/PKB mRNA in the coinjection experiment, we were able to generate more intersegmental vessels

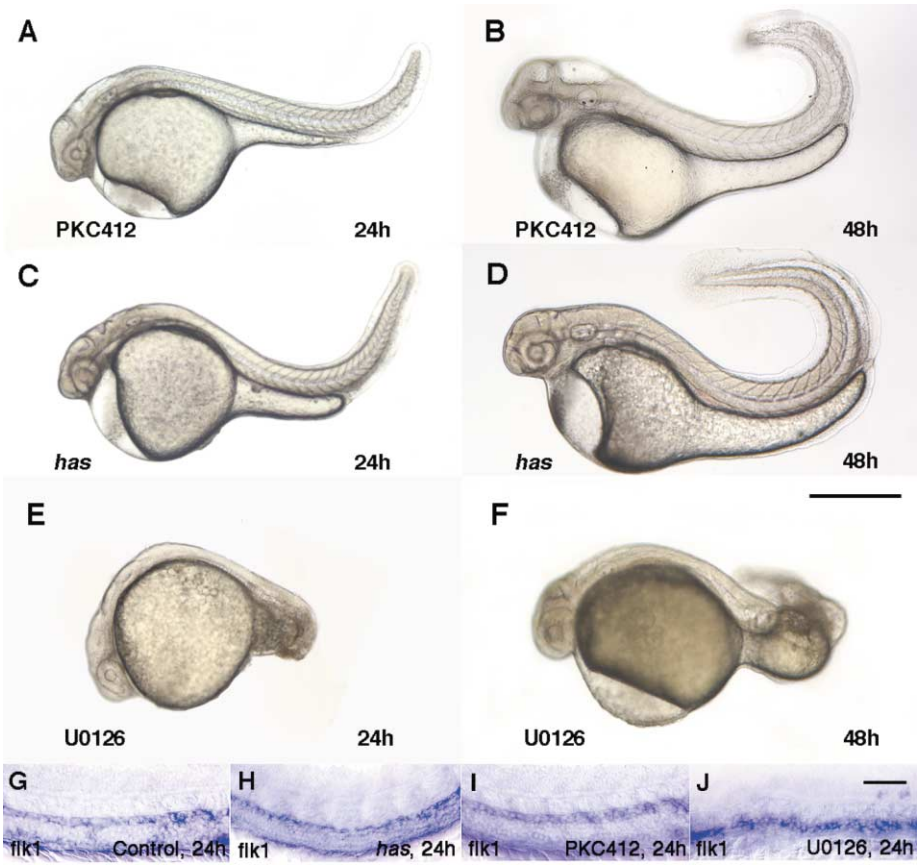

Figure 7. Serine/threonine kinase inhibitors can phenocopy known in vivo defects

A–D: Zebrafish embryos treated with 100 nM PKC412 at shield stage (6 hpf, **A** and **B**) generated a curved body axis similar to the genetic mutant, *heart-and-soul* (*has*), at 24 hpf and 48 hpf (**C** and **D**). **E and F:** Embryos treated with 100 μM of U0126 at shield stage (6 hpf) displayed a loss of posterior structures. **G–J:** In situ RNA staining with an endothelial marker indicates the presence of *flk-1* positive cells in the control, *has*, PKC412-treated, and U0126-treated embryos at 24 hpf. Scale bars for **A–F** = 500 μm; **G–J** = 100 μm.

at 48 hpf, compared with embryos injected with the lowered VEGF-A morpholino alone (Table 1).

Inevitably the system will fail to assess some compounds correctly. For instance the zebrafish homolog of the c-Kit receptor is well conserved, and yet STI571, a potent inhibitor of the both c-Abl and c-Kit kinases, fails to phenocopy a genetic c-*kit* mutation (Parichy et al., 1999) or indeed have any effect on zebrafish development (J.C. and T.M.R., unpublished data). However, our experience to date suggests that the zebrafish system will be useful in evaluating many signaling drugs. In particular, we suggest that the zebrafish system can play a useful role as an initial animal screen before investment in more costly and time-consuming rodent studies.

No model system is perfect, but the zebrafish system offers a unique combination of advantages that strengthen its potential as a prescreen model for drug evaluation. It is inexpensive; at less than 1% of the cost of maintaining mice, the number of embryos available for drug treatment can be much higher. As the sample numbers increase, statistical confidence in the outcome of the experiment improves. Equally importantly, the amount of a compound required is small. In the course of this study we tested over 30,000 animals, with less than 5 mg of PTK787/ZK222584 for the entire study.

The sequencing of the human genome has revealed an extremely large number of potential targets for drug design. However, candidate drugs require extensive testing in model animals. Current mammalian models are expensive to house and time-consuming to use. The zebrafish can provide a cost-efficient and quick system for a prescreen. A single person can generate thousands of animals and test numerous compounds on a daily basis. The rapid development of the transparent zebrafish embryo permits easy visual analysis of phenotypic defects. In addition, accumulating genetic data from zebrafish mutants will provide a growing database for phenotypic comparison of functional loss in a given signaling pathway.

Experimental procedures

Maintenance of zebrafish and drug treatments

Breeding fish were maintained at 28.5°C on a 14 hr light/10 hr dark cycle. Embryos were collected by natural spawning, raised in 10% Hank's saline, and staged up to 24 hr (30 somites) according to Kimmel et al. (1995); beyond this point, embryo stage is given as hours post fertilization (hpf). Kinase inhibitors, PTK787/ZK222584, and PKC412 (Novartis Pharma AG, Basel, Switzerland), were dissolved in DMSO at stock concentrations of 2 mM; U0126 (Promega) was dissolved at 50 mM in DMSO, then diluted in embryo media (Westerfield, 1995) and added to live zebrafish embryos at the stages indicated. Control embryos were treated with the equivalent amount of DMSO solution. All embryos are incubated at 28.5°C.

Isolation and characterization of cDNA clones for VEGFR-2 and AKTβ/PKB-2

The cDNAs encoding rat EphA8 receptor tyrosine kinase domain (Chan and Watt, 1991) and the human AKT-1/PKB-α (Ramaswamy et al., 1999) were used to screen an 18 hr zebrafish embryonic cDNA library at low stringency (Chan et al., 2001). Full-length cDNA clones were isolated encoding zebrafish VEGFR-2/flk-1/KDR receptor and AKT-2/PKBβ: *VEGFR-2*, *AKT-2/PKB*β (GenBank accession numbers: AY056466, AY056465, respectively). Nucleotide sequences were determined using the dideoxy method by the Dana-Farber Cancer Institute Molecular Biology Core Facility.

Mammalian cell culture and biochemical analysis

COS-7 cells were maintained at 5% CO_2 in Dulbucco's modified Eagle's medium (DMEM) supplemented with 10% fetal bovine serum. Zebrafish full-length cDNAs encoding VEGF-A (Liang et al., 1998) and VEGFR-2/flk-1 were cloned into mammalian expression vectors pCS2+ (Turner and Weintraub, 1994) and pBK-CMV (Stratagene), respectively, and transfected (10 μg DNA) into COS-7 cells using Fugene-6 as per the manufacturer's instructions (Roche). At 48 hr posttransfection, receptor-expressing cells were serum starved for 16 hr at 0.5% fetal bovine serum in DMEM media. For PTK787/ZK222584 treatment, receptor-expressing cells were preincubated with various concentrations of PTK787/ZK222584 for 2 hr at 37°C before ligand stimulation. The supernatant was first removed from the zebrafish VEGFR-2-expressing cells, then replaced with supernatant from the ligand-expressing cells and incubated for 15 min before lysis (NP-40 lysis buffer: 20 mM TRIS (pH8), 137 mM NaCl, 1% Nonidet P-40, 10% glycerol, 1 mM PMSF, 1 mM sodium vanadate, 100 μM NaF, 10 μg/ml aprotinin, 5 μg/ml Pepstatin, 5 μg/ml leupeptin). Lysates were immunoprecipitated with the monoclonal phosphotyrosine antibody 4G10 (Upstate Biotechnology), separated on a 7.5% SDS-PAGE gel, then immunoblotted with the same antibody. Tyrosine phosphorylated proteins were visualized using enhanced chemiluminence (ECL, Amersham).

RNA in situ hybridization

Whole-mount zebrafish in situ hybridization using various digoxigenin-labeled antisense RNA probes was performed using standard methods as previously described (Chan et al., 2001). RNA probes containing digoxigenin-11-UTP (Roche) were visualized using the BM purple alkaline phosphatase substrate (Roche). Embryos were cleared and flat-mounted in 70% glycerol for photography.

JB-4 plastic sections

Zebrafish whole-mount embryos were fixed overnight in 4% paraformaldehyde in PBS and dehydrated in ethanol and infiltrated in JB-4 infiltration resin following the manufacturer's instructions (Polysciences Inc., Warrington, Pennsylvania). Specimens were sectioned at 5 μm using a Jung Supercut 2065 microtome. Histological hematoxylin-eosin and 0.1% aqueous Azure II staining of the sections was subsequently carried out using standard protocols.

Microinjections

Myristoylated form of the human AKT-1/PKBα cDNA (Ramaswamy et al., 1999) or bovine eNOS cDNAs (Fulton et al., 1999) were linearized at the 3′ end, and capped RNAs were in vitro transcribed using the Message Machine Kit (Ambion Inc., Austin, Texas), following the manufacturer's instructions. A volume of 2 nanoliters of various mRNAs was microinjected into one-cell stage zebrafish embryos using a gas driven microinjector (Medical Systems Corp., Greenvale, New York). Low concentrations of mRNAs were chosen for vessel rescue as determined by titration experiments. Each mRNA was used at concentrations below the threshold for generating morphological defects: AKT/PKB mRNAs at 50 ng/μl; eNOS mRNAs at 75 ng/μl; control GFP mRNA at 50 ng/μl. The VEGF-A ligand morpholino, same sequence as VEGF-A-3 (Nasevicius et al., 2000), was injected at 75 μM, and coinjection with AKT/PKB mRNA was used at 25 ng/μl.

Microangiography

Live zebrafish embryo microangiography was performed essentially as described (Weinstein et al., 1995). Fluorescein lectin, Alexa Flour® 488 conjugate (Molecular Probes, Eugene, Oregon) 5 mg/ml in Danieau's solution (58 mM NaCl, 0.7 mM KCl, 0.4 mM $MgSO_4$, 0.6 mM $Ca(NO_3)_2$, 5 mM HEPES [pH 7.6]) was injected into the sinus venosa/cardinal vein of the anaesthetized zebrafish embryo at 48 hpf and the photography was performed on a Nikon Eclipse E600 microscope.

Whole-mount TUNEL staining

For whole-mount TUNEL staining, embryos were fixed in 4% paraformaldehyde at 4°C overnight, then rinsed in phosphate-buffered saline before proceeding with TUNEL staining using the ApopTag® Peroxidase In situ Apoptosis Detection kit (Intergen Co., Purchase, New York) as per the manufacturer's instructions, essentially as previously described (Abdelilah et al., 1996).

Acknowledgments

We thank Mark Fishman for the zebrafish *heart and soul* mutant, Bill Sellers for the human *AKT-1/PKBα* constructs, Bill Sessa for the endothelial nitric oxide synthase constructs, Len Zon for the *fli-1* and *flt4* plasmids, Ruowen Ge for the *VEGF-A* cDNA, Fabrizio Serluca for the *wt1* plasmid, Alan Mayer for the *insulin*, *trypsin* plasmids, and Jau-Nian Chen for the *fkd2* plasmid. We are grateful to Fabrizio Serluca and Mark Fishman for communicating results before publication. We thank John Mably, Fabrizio Serluca, Randall Peterson, David Livingston, Tony Pawson, and Colin Bayliss for helpful discussions and/or critical reading of the manuscript. We acknowledge Matthew Thomas and Nathan Goldstein for technical assistance. This work was supported by NIH grants to T.M.R. (HD24926, CA30002, CA89021). In compliance with Harvard Medical School guidelines on possible conflict of interest, we disclose that one of the authors (T.M.R.) has consulting relationships with Upstate Biotechnology and Novartis Pharmaceuticals, Inc.

Received: November 29, 2001
Revised: March 19, 2001

References

Abdelilah, S., Mountcastle-Shah, E., Harvey, M., Solnica-Krezel, L., Schier, A.F., Stemple, D.L., Malicki, J., Neuhauss, S.C., Zwartkruis, F., Stainier, D.Y., et al. (1996). Mutations affecting neural survival in the zebrafish Danio rerio. Development *123*, 217–227.

Argenton, F., Zecchin, E., and Bortolussi, M. (1999). Early appearance of pancreatic hormone-expressing cells in the zebrafish embryo. Mech. Dev. *87*, 217–221.

Biemar, F., Argenton, F., Schmidtke, R., Epperlein, S., Peers, B., and Driever, W. (2001). Pancreas development in zebrafish: early dispersed appearance of endocrine hormone expressing cells and their convergence to form the definitive islet. Dev. Biol. *230*, 189–203.

Bold, G., Altmann, K.H., Frei, J., Lang, M., Manley, P.W., Traxler, P., Wietfeld, B., Bruggen, J., Buchdunger, E., Cozens, R., et al. (2000). New anilinophthalazines as potent and orally well absorbed inhibitors of the VEGF receptor tyrosine kinases useful as antagonists of tumor-driven angiogenesis. J. Med. Chem. *43*, 2310–2323.

Carmeliet, P. (2000). Mechanisms of angiogenesis and arteriogenesis. Nat. Med. *6*, 389–395.

Carmeliet, P., and Jain, R.K. (2000). Angiogenesis in cancer and other diseases. Nature *407*, 249–257.

Chan, J., and Watt, V.M. (1991). eek and erk, new members of the eph subclass of receptor protein-tyrosine kinases. Oncogene *6*, 1057–1061.

Chan, J., Mably, J.D., Serluca, F.C., Chen, J.N., Goldstein, N.B., Thomas, M.C., Cleary, J.A., Brennan, C., Fishman, M.C., and Roberts, T.M. (2001). Morphogenesis of prechordal plate and notochord requires intact Eph/ephrin B signaling. Dev. Biol. *234*, 470–482.

Chen, J.N., van Bebber, F., Goldstein, A.M., Serluca, F.C., Jackson, D., Childs, S., Serbedzija, G., Warren, K.S., Mably, J.D., Lindahl, P., et al. (2001). Genetic steps to organ laterality in zebrafish. Comp. Funct. Genom. *2*, 60–68.

Dimmeler, S., Fleming, I., Fisslthaler, B., Hermann, C., Busse, R., and Zeiher, A.M. (1999). Activation of nitric oxide synthase in endothelial cells by Akt-dependent phosphorylation. Nature *399*, 601–605.

Drevs, J., Hofmann, I., Hugenschmidt, H., Wittig, C., Madjar, H., Muller, M., Wood, J., Martiny-Baron, G., Unger, C., and Marme, D. (2000). Effects of PTK787/ZK 222584, a specific inhibitor of vascular endothelial growth factor receptor tyrosine kinases, on primary tumor, metastasis, vessel density, and blood flow in a murine renal cell carcinoma model. Cancer Res. *60*, 4819–4824.

Ekker, S.C. (2000). Morphants: a new systematic vertebrate functional genomics approach. Yeast *17*, 302–306.

Favata, M.F., Horiuchi, K.Y., Manos, E.J., Daulerio, A.J., Stradley, D.A.,

Feeser, W.S., Van Dyk, D.E., Pitts, W.J., Earl, R.A., Hobbs, F., et al. (1998). Identification of a novel inhibitor of mitogen-activated protein kinase kinase. J. Biol. Chem. *273*, 18623–18632.

Ferrara, N., and Alitalo, K. (1999). Clinical applications of angiogenic growth factors and their inhibitors. Nat. Med. *5*, 1359–1364.

Fishman, M.C. (2001). Genomics. Zebrafish—the canonical vertebrate. Science *294*, 1290–1291.

Fouquet, B., Weinstein, B.M., Serluca, F.C., and Fishman, M.C. (1997). Vessel patterning in the embryo of the zebrafish: guidance by notochord. Dev. Biol. *183*, 37–48.

Fujio, Y., and Walsh, K. (1999). Akt mediates cytoprotection of endothelial cells by vascular endothelial growth factor in an anchorage-dependent manner. J. Biol. Chem. *274*, 16349–16354.

Fulton, D., Gratton, J.P., McCabe, T.J., Fontana, J., Fujio, Y., Walsh, K., Franke, T.F., Papapetropoulos, A., and Sessa, W.C. (1999). Regulation of endothelium-derived nitric oxide production by the protein kinase Akt. Nature *399*, 597–601.

Gerber, H.P., McMurtrey, A., Kowalski, J., Yan, M., Keyt, B.A., Dixit, V., and Ferrara, N. (1998). Vascular endothelial growth factor regulates endothelial cell survival through the phosphatidylinositol 3′-kinase/Akt signal transduction pathway. Requirement for Flk-1/KDR activation. J. Biol. Chem. *273*, 30336–30343.

Horne-Badovinac, S., Lin, D., Waldron, S., Schwarz, M., Mbamalu, G., Pawson, T., Jan, Y., Stainier, D.Y., and Abdelilah-Seyfried, S. (2001). Positional cloning of heart and soul reveals multiple roles for PKC lambda in zebrafish organogenesis. Curr. Biol. *11*, 1492–1502.

Isogai, S., Horiguchi, M., and Weinstein, B.M. (2001). The vascular anatomy of the developing zebrafish: an atlas of embryonic and early larval development. Dev. Biol. *230*, 278–301.

Jiang, B.H., Zheng, J.Z., Aoki, M., and Vogt, P.K. (2000). Phosphatidylinositol 3-kinase signaling mediates angiogenesis and expression of vascular endothelial growth factor in endothelial cells. Proc. Natl. Acad. Sci. USA *97*, 1749–1753.

Kimmel, C.B., Ballard, W.W., Kimmel, S.R., Ullmann, B., and Schilling, T.F. (1995). Stages of embryonic development of the zebrafish. Dev. Dyn. *203*, 253–310.

Lammert, E., Cleaver, O., and Melton, D. (2001). Induction of pancreatic differentiation by signals from blood vessels. Science *294*, 564–567.

Lewandoski, M. (2001). Conditional control of gene expression in the mouse. Nat. Rev. Genet. *2*, 743–755.

Liang, D., Xu, X., Chin, A.J., Balasubramaniyan, N.V., Teo, M.A., Lam, T.J., Weinberg, E.S., and Ge, R. (1998). Cloning and characterization of vascular endothelial growth factor (VEGF) from zebrafish, Danio rerio. Biochim. Biophys. Acta *1397*, 14–20.

Liao, W., Bisgrove, B.W., Sawyer, H., Hug, B., Bell, B., Peters, K., Grunwald, D.J., and Stainier, D.Y. (1997). The zebrafish gene cloche acts upstream of a flk-1 homologue to regulate endothelial cell differentiation. Development *124*, 381–389.

MacNicol, A.M., Muslin, A.J., and Williams, L.T. (1993). Raf-1 kinase is essential for early Xenopus development and mediates the induction of mesoderm by FGF. Cell *73*, 571–583.

Matsumoto, K., Yoshitomi, H., Rossant, J., and Zaret, K.S. (2001). Liver organogenesis promoted by endothelial cells prior to vascular function. Science *294*, 559–563.

Meyer, T., Regenass, U., Fabbro, D., Alteri, E., Rosel, J., Muller, M., Caravatti, G., and Matter, A. (1989). A derivative of staurosporine (CGP 41 251) shows selectivity for protein kinase C inhibition and in vitro anti-proliferative as well as in vivo anti-tumor activity. Int. J. Cancer *43*, 851–856.

Milewski, W.M., Duguay, S.J., Chan, S.J., and Steiner, D.F. (1998). Conservation of PDX-1 structure, function, and expression in zebrafish. Endocrinology *139*, 1440–1449.

Mills, A.A. (2001). Changing colors in mice: an inducible system that delivers. Genes Dev. *15*, 1461–1467.

Morales-Ruiz, M., Fulton, D., Sowa, G., Languino, L.R., Fujio, Y., Walsh, K., and Sessa, W.C. (2000). Vascular endothelial growth factor-stimulated actin reorganization and migration of endothelial cells is regulated via the serine/threonine kinase Akt. Circ. Res. *86*, 892–896.

Nasevicius, A., and Ekker, S.C. (2000). Effective targeted gene 'knockdown' in zebrafish. Nat. Genet. *26*, 216–220.

Nasevicius, A., Larson, J., and Ekker, S.C. (2000). Distinct requirements for zebrafish angiogenesis revealed by a VEGF-A morphant. Yeast *17*, 294–301.

Ozaki, H., Seo, M.S., Ozaki, K., Yamada, H., Yamada, E., Okamoto, N., Hofmann, F., Wood, J.M., and Campochiaro, P.A. (2000). Blockade of vascular endothelial cell growth factor receptor signaling is sufficient to completely prevent retinal neovascularization. Am. J. Pathol. *156*, 697–707.

Parichy, D.M., Rawls, J.F., Pratt, S.J., Whitfield, T.T., and Johnson, S.L. (1999). Zebrafish sparse corresponds to an orthologue of c-kit and is required for the morphogenesis of a subpopulation of melanocytes, but is not essential for hematopoiesis or primordial germ cell development. Development *126*, 3425–3436.

Peterson, R.T., Link, B.A., Dowling, J.E., and Schreiber, S.L. (2000). Small molecule developmental screens reveal the logic and timing of vertebrate development. Proc. Natl. Acad. Sci. USA *97*, 12965–12969.

Peterson, R.T., Mably, J.D., Chen, J.N., and Fishman, M.C. (2001). Convergence of distinct pathways to heart patterning revealed by the small molecule concentramide and the mutation heart-and-soul. Curr. Biol. *11*, 1481–1491.

Ramaswamy, S., Nakamura, N., Vazquez, F., Batt, D.B., Perera, S., Roberts, T.M., and Sellers, W.R. (1999). Regulation of G1 progression by the PTEN tumor suppressor protein is linked to inhibition of the phosphatidylinositol 3-kinase/Akt pathway. Proc. Natl. Acad. Sci. USA *96*, 2110–2115.

Roy, S., Qiao, T., Wolff, C., and Ingham, P.W. (2001). Hedgehog signaling pathway is essential for pancreas specification in the zebrafish embryo. Curr. Biol. *11*, 1358–1363.

Rubin, G.M. (1991). Signal transduction and the fate of the R7 photoreceptor in Drosophila. Trends Genet. *7*, 372–377.

Serluca, F.C., and Fishman, M.C. (2001). Pre-pattern in the pronephric kidney field of zebrafish. Development *128*, 2233–2241.

Serluca, F.C., Drummond, I.A., and Fishman, M.C. (2002) Endothelial signaling in kidney morphogenesis: A role for hemodynamic forces. Curr. Biol. *12*, 492–497.

Simon, M.A., Bowtell, D.D., Dodson, G.S., Laverty, T.R., and Rubin, G.M. (1991). Ras1 and a putative guanine nucleotide exchange factor perform crucial steps in signaling by the sevenless protein tyrosine kinase. Cell *67*, 701–716.

Smith, E.A., Seldin, M.F., Martinez, L., Watson, M.L., Choudhury, G.G., Lalley, P.A., Pierce, J., Aaronson, S., Barker, J., Naylor, S.L., et al. (1991). Mouse platelet-derived growth factor receptor alpha gene is deleted in W19H and patch mutations on chromosome 5. Proc. Natl. Acad. Sci. USA *88*, 4811–4815.

Stainier, D.Y., Fouquet, B., Chen, J.N., Warren, K.S., Weinstein, B.M., Meiler, S.E., Mohideen, M.A., Neuhauss, S.C., Solnica-Krezel, L., Schier, A.F., et al. (1996). Mutations affecting the formation and function of the cardiovascular system in the zebrafish embryo. Development *123*, 285–292.

Stephenson, D.A., Mercola, M., Anderson, E., Wang, C.Y., Stiles, C.D., Bowen-Pope, D.F., and Chapman, V.M. (1991). Platelet-derived growth factor receptor alpha-subunit gene (Pdgfra) is deleted in the mouse patch (Ph) mutation. Proc. Natl. Acad. Sci. USA *88*, 6–10.

Sternberg, P.W. (1993). Intercellular signaling and signal transduction in C. elegans. Annu. Rev. Genet. *27*, 497–521.

Sternberg, P.W., and Horvitz, H.R. (1991). Signal transduction during C. elegans vulval induction. Trends Genet. *7*, 366–371.

Sumoy, L., Keasey, J.B., Dittman, T.D., and Kimelman, D. (1997). A role for notochord in axial vascular development revealed by analysis of phenotype and the expression of VEGR-2 in zebrafish flh and ntl mutant embryos. Mech. Dev. *63*, 15–27.

Thisse, C., and Zon, L.I. (2002). Organogenesis—heart and blood formation from the zebrafish point of view. Science *295*, 457–462.

Thompson, M.A., Ransom, D.G., Pratt, S.J., MacLennan, H., Kieran, M.W., Detrich, H.W., 3rd, Vail, B., Huber, T.L., Paw, B., Brownlie, A.J., et al. (1998). The cloche and spadetail genes differentially affect hematopoiesis and vasculogenesis. Dev. Biol. *197*, 248–269.

Turner, D.L., and Weintraub, H. (1994). Expression of achaete-scute homolog 3 in Xenopus embryos converts ectodermal cells to a neural fate. Genes Dev. *8*, 1434–1447.

Weinstein, B.M., Stemple, D.L., Driever, W., and Fishman, M.C. (1995). Gridlock, a localized heritable vascular patterning defect in the zebrafish. Nat. Med. *1*, 1143–1147.

Wen, S., Stolarov, J., Myers, M.P., Su, J.D., Wigler, M.H., Tonks, N.K., and Durden, D.L. (2001). PTEN controls tumor-induced angiogenesis. Proc. Natl. Acad. Sci. USA *98*,4622–4627.

Westerfield, M. (1995). The Zebrafish Book: Guide for the Laboratory Use of Zebrafish (Danio rerio). (Eugene, Oregon: University of Oregon Press).

Wood, J.M., Bold, G., Buchdunger, E., Cozens, R., Ferrari, S., Frei, J., Hofmann, F., Mestan, J., Mett, H., O'Reilly, T., et al. (2000). PTK787/ZK 222584, a novel and potent inhibitor of vascular endothelial growth factor receptor tyrosine kinases, impairs vascular endothelial growth factor-induced responses and tumor growth after oral administration. Cancer Res. *60*, 2178–2189.

Accession numbers

The GenBank accession numbers for zebrafish *VEGFR-2* and *AKT-2/PKB* are AY056466 and AY056465, respectively.